Proceedings of the XI DINAME, 28th February-4th March, 2005 - Ouro Preto - MG - Brazil
Edited by D.A. Rade and V. Steffen Jr.

DYNAMIC ANALYSIS OF SILICON MICROMACHINED DOUBLE-ROTOR SCANNING MIRROR

L. C. M. Oliveira
Dept. of Computational Mechanics - FEM - UNICAMP - Av. Mendeleiev, S/N - 13083-970 - Campinas - SP - Brazil
marangoni@fem.unicamp.br

K. M. Ahmida
Center for Semiconductor Components CCS - UNICAMP - P. O. Box 6061 - 13083-970 - Campinas - SP - Brazil
khaled@fem.unicamp.br

L. O. S. Ferreira
Dept. of Computational Mechanics - FEM - UNICAMP - Av. Mendeleiev, S/N - 13083-970 - Campinas - SP - Brazil
lotavio@fem.unicamp.br

Abstract: *The use of MEMS-based technologies for producing scanning mirrors enables its batch production with a consequent increase in the throughput and a decrease in the manufacturing costs per device. However, the use of Silicon as a structural material introduces non-linearities in the device behavior due to the variation of its mechanical properties according to the crystalline orientation. In this way, the use of finite elements based methods in the device modeling enhances greatly the accuracy in the design of micromachined scanning mirrors. To validate the finite element model, a modal analysis of the device was performed using the Laser Doppler Vibrometry method. The normal modes of the structure were identified and the results agree well with the model. This work presents the FE model and experimental modal analysis results of a Silicon micromachined double-rotor scanning mirror.*

Keywords: *Microscanners, torsional oscillators, modal analysis, Laser doppler vibrometry, FEA*

1. Introduction

In the field of optomechatronic systems, scanning mirrors or scanners have gathered a significant attention, since they are a fundamental element of a wide variety of devices, such as barcode readers, confocal microscopes and laser printers (Wu, 1997; Urbach et al., 1982; Miyajima et al., 2003). Scanners project laser beams that are used, for example, to produce images by raster scanning or collect images in confocal microscopy. Large area (mm order) devices, as the one presented in this work, have a broad spectrum of specific applications where the power of the laser beam and/or the optical aperture are a requirement for the system. In this context, the micromachined scanners competes directly with the galvanometric scanners (Zeleny, 2004) that are fine and precise mechanical devices whose prices are on the hundred of dollars range. Silicon mm-size micromachined scanning mirrors are an alternative to such devices. The structure usually adopted in scanners consists of a single rotor devoted both to actuation and light beam deflection. The device presented in this work is a double-rotor scanner (Oliveira and Ferreira, 2003) where the basic idea is the separation between the actuation and the mirror mechanisms in order to improve the performance of each one separately, fig. 1.

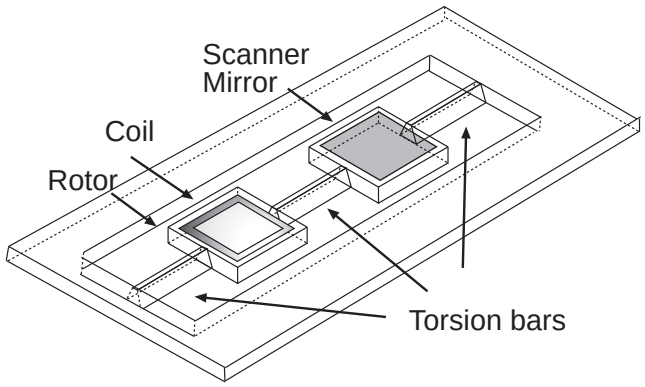

Figure 1: Double-rotor scanner geometry. The structure consists of two square rotors linked to a fixed frame by two torsion bars, a third torsion bar connect both rotors.

In the field of scanners some of the most important parameters are the frequency and amplitude of the torsional modes of the structure. These are the operational modes of the device and have to be enhanced in order to improve the device performance. The identification of the other modes is important due to their influence in the device operation. Such modes are responsible for the noise and must be reduced or have their frequency translated to frequencies that do not influence the device operation in a significant way.

The presented device was prototyped using Microelectromechanical (MEMS) fabrication process. The use of such technology in its production makes possible the batch fabrication of such devices with a potential decrease in the fabrication costs due to the scale of production. On the other hand, the use of Silicon as a structural material introduces non-linearities in the device behavior due to the variation of its mechanical properties according to the crystalline orientation. In this way, the use of finite elements based methods in the device modeling enhances greatly the accuracy in the design of micromachined scanning mirrors.

In this work a structural FE of double-rotor scanner was developed and its main dynamic parameters were obtained. To validate such results two experiments were carried out, first the frequency response of the device was obtained and then the main vibrational modes of the structure were identified by a laser doppler vibrometry experiment. The model predicted results that are in good agreement with the experimental ones.

2. Scanning Mirror Fabrication

The devices were made using bulk micromachinning of Silicon (Kovacs et al., 1998), thin film and mechanical assembly techniques. As substrate, a Silicon single-crystal 2" diameter, $< 100 >$, $200\mu m$ thick, was used. A $1.30\mu m$ SiO_2 film was thermally grown and lithographed.

The micromachinning process was based on the anisotropic etching of $< 100 >$ Si wafer, using Potassium Hydroxide (KOH) as selective etchant (Seidel et al., 1990b; Seidel et al., 1990a; Williams and Muller, 1996). The fabrication process is described in fig. 2

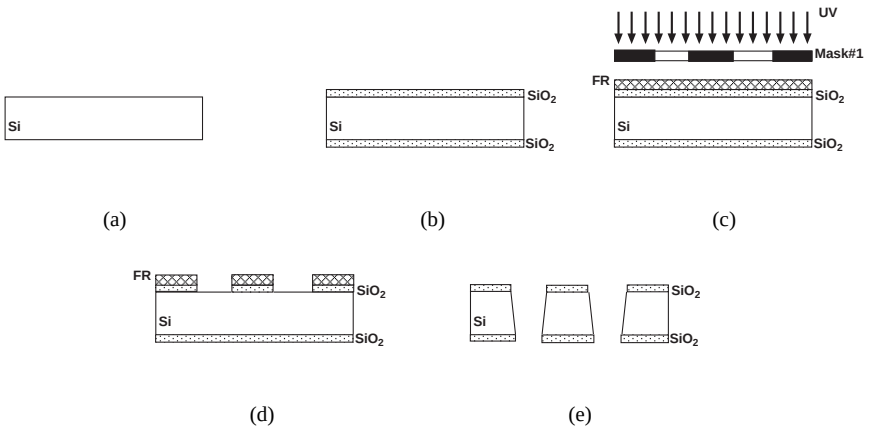

Figure 2: Scanner fabrication process (a) Si wafer (b) Growing of 1.30μ SiO2 film (c) FR (Fotoresist) UV exposure (d) FR Development (e) KOH etching

The cooper coil was patterned separately and transferred to the silicon surface by mechanical assembly. Prototypes fabrication can be greatly enhanced by using this technique instead of conventional thin film techniques.

Figure 3 shows details of the fabricated devices. Figure 3(a) presents the trapezoidal profile of the torsion bar. A rotor´s convex corner is shown in fig.3(b) demonstrating the efficiency of the corner compensation structures adopted.

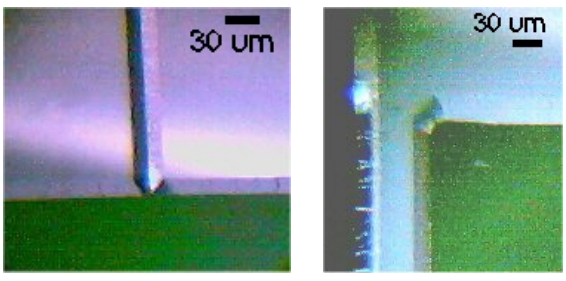

Figure 3: Fabricated scanner details (a) torsion bar (b) Convex corner

Figure 4 shows the whole device and tab.1 its main dimensions. The packaging used was a PMMA (Poly-Methyl-Meta-Acrylate) support specially designed to accommodate the scanner.

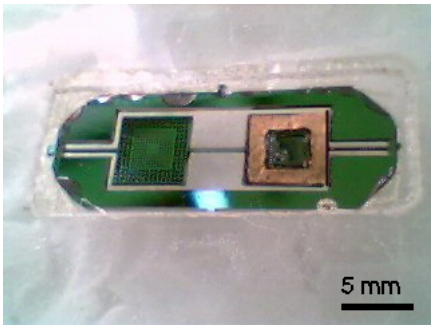

Figure 4: Fabricated device.

Table 1: Scanner dimensions.

Scanner total size [mm]	23 x 8.5
Mirror size [mm]	5 x 5
Rotor size [mm]	5 x 5
Coil lateral lenght [mm]	4 x 4
Torsion bars width [μm]	100
Torsion bars length [mm]	4

3. FEA Modeling

To analyze the dynamic behavior of the double-rotor scanner structure a 3D finite elements analysis was conducted using the general purpose finite element package ANSYS®. Two kinds of analyzes were performed. As a first step, a modal analysis was used to identify the natural frequencies and mode shapes of the structure, where the torsional mode shapes of the scanner and their respective natural frequencies were found. As a second step, the harmonic analysis was conducted to determine the steady-stead response of the scanner with a load that varies sinusoidally (harmonically) with time.

The device was modeled using Solid45 finite element, see fig. 5. This element is defined by eight nodes having three degrees of freedom on each node: translations in the nodal x-, y- and z-direction. A regular pattern (mapped mesh) was generated using only hexahedrons. Table 2 presents the main simulation parameters.

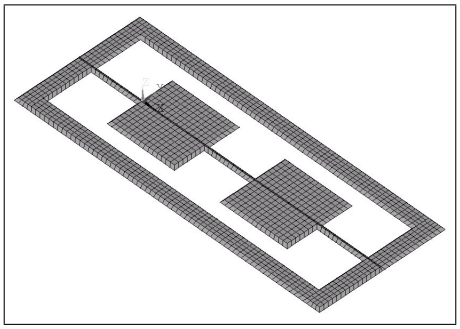

Figure 5: FEA model of the double-rotor scanner

In this model Silicon was supposed to be isotropic and its properties are in tab. 3. In a next step an orthotropic model will be used in order to improve the model accuracy.

Table 2: Parameters for the FEA model

Elements and mesh	
Element	Solid45
DOFs	UX, UY, UZ
Element size	$1.8mm$
Number of elements/nodes	1290/3100

Table 3: Silicon Properties adopted in the FEA model(Petersen, 1980)

Bulk Silicon Properties	
Density	$2330Kg/m^3$
Young´s modulus	$45GPa$
Poisson ratio	0.09

The FEA modal analysis shows the first five modes of the double-rotor scanner structure. From these results we can identify the torsional modes of the structure, in this case the 3^{rd} and the 5^{th}. These modes are the main modes of the device and can be easily identified experimentally.

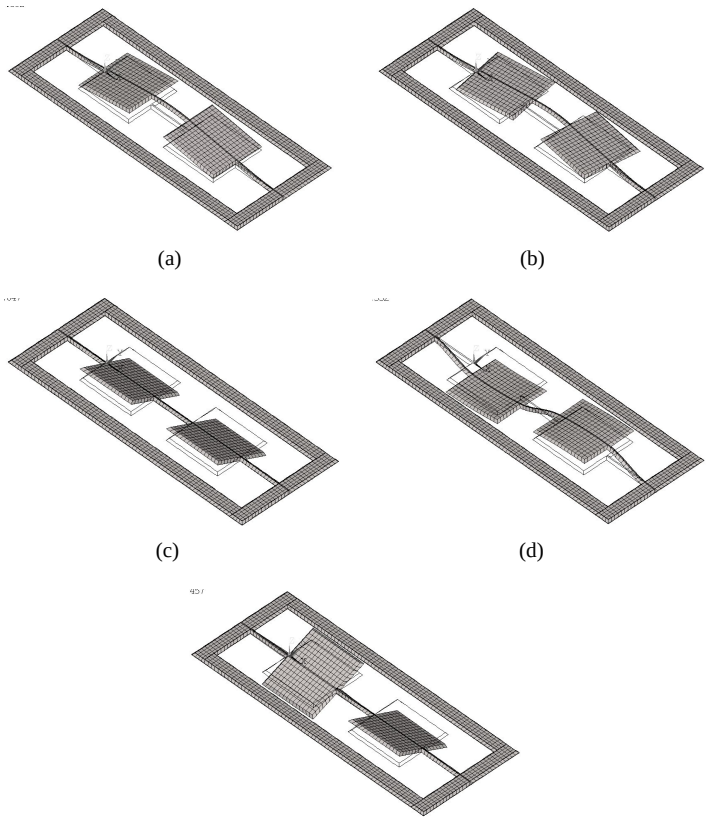

(a) (b) (c) (d) (e)

Figure 6: FEA predict modes (a) 1^{st} mode - 677 Hz (b) 2^{nd} mode - 1130 Hz (c) 3^{rd} mode (torsional) - 1595 Hz (d) 4^{th} mode - 2528 Hz (e) $5^{th}mode$ - (torsional) - 2766 Hz

4. Experimental Characterization

In order to validate the FEA results two experiments were performed. First, a setup was developed to get the frequency response of the device. In this way the frequency and amplitude of the main torsional modes could be obtained. Then, a laser doppler vibrometry was done to perform a modal identification. These experiments are explained in the following sections.

4.1. Frequency response

Figure 7 presents a schematic view of the measurement setup used in the device characterization. A laser beam from a laser diode is reflected by the mirror and directed to a semiconductor position sensitive device, PSD, which generates an electric signal proportional to the deflection of the laser beam. This output signal is read by the acquisition system that generates the scanner response.

The acquisition system is composed by a function generator and by a digital oscilloscope. An interface based on the *Vee Pro*® software was specifically developed to control the instrumentation and to automatize the measurements. The interface changes linearly the frequency of the AC magnetic field B_2 generated by the magnetic circuit and reads the electric output signal generated by a PSD (Position Sensitive Detector) proportional to the scan deflection.

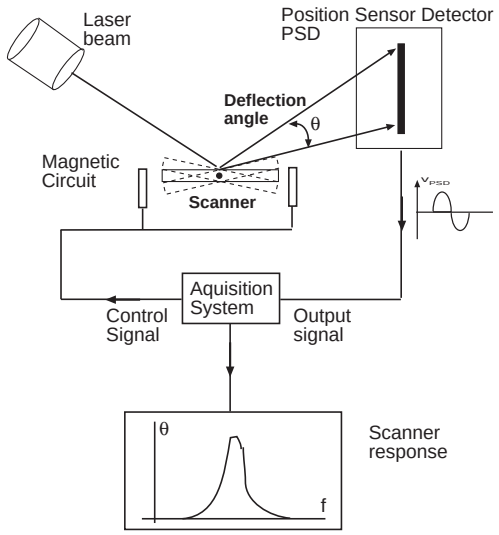

Figure 7: Schematic view of the characterization setup.

Figure 8 shows the measured scanner frequency response. A typical second-order system response with resonant frequencies of $1316Hz$ and $2542Hz$ was obtained.

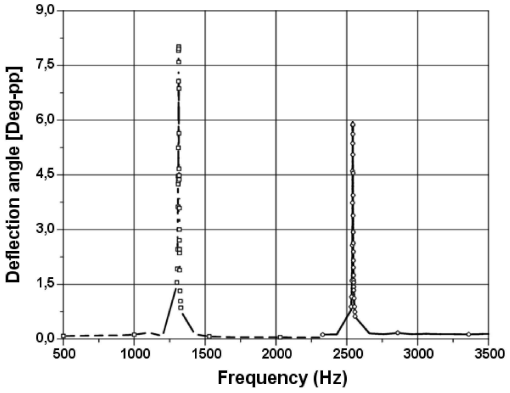

Figure 8: Deflection angle vs. drive frequency for the double-rotor scanner. See the two resonant frequencies of 1316 Hz and 2542 Hz, according to the model.

The resonant frequency peaks are presented in detail in fig. 9. The double-rotor scanner show a maximum deflection angle of $8^o pp$ at the first peak, $1316Hz$, as can be see in fig. 9(a). This result is compatible with the result of $10^o pp$ obtained in a previous work about silicon induction actuated scanners(Barbaroto, 2002). This deflection angle can be improved by optimizing the geometry of the scanner´s mirror or improving the coupling between the magnetic circuit and the scanner´s coil.

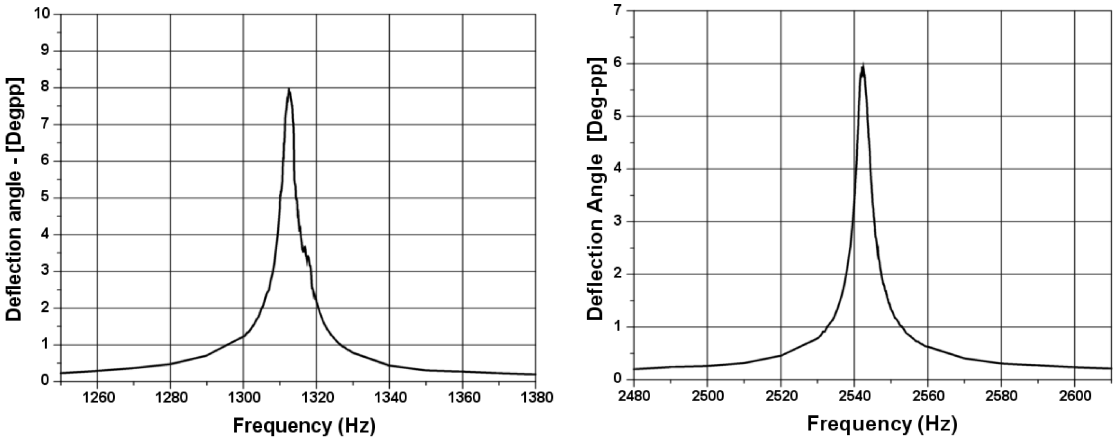

(a) (b)

Figure 9: Scanner frequency response at (a) 1316 Hz (b) 2542 Hz

Table 4.1 presents a summary of the results obtained in the device characterization.

Table 4: Summary of the double-rotor frequency response results.

First resonance frequency [Hz]	1316
Quality factor (First peak)	200
Scan angle [Deg pp]	8
Second resonance frequency [Hz]	2542
Quality factor (Second peak)	422
Scan angle [Deg pp]	6

4.2. Laser Doppler Vibrometry

The numerical results obtained via the finite element analysis were validated experimentally. An excitation chirp signal, in the range of 1 Hz to 4 kHz with 0.5Hz resolution, was sent to the rotor and was used as the reference signal. The out-of-plane velocity of the scanner surface was measured with a laser Doppler vibrometer (Polytec OFV 330) aiming the laser beam orthogonal to its surface. The excitation and the response signals were acquired using the HP-VXI data acquisition system and LMS CADA-X® software package, fig.10(b). The Measurements were taken at 23 locations on the surface of the double-rotor scanner, as shown in fig. 10(a).

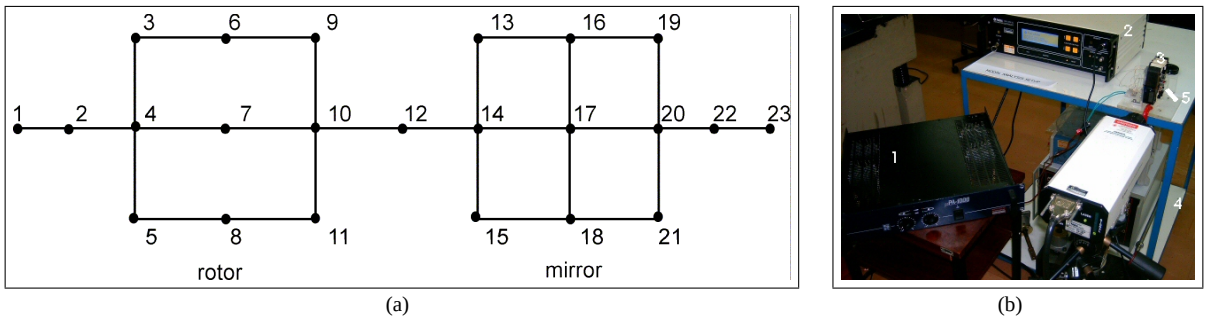

(a) (b)

Figure 10: Laser Doppler Vibrometry settings (a) Measurement points (b) Experimental Setup

The experimental modal analysis resulted in the following mode shapes and natural frequencies. The first five mode shapes of the scanner were identified using the measured FRFs and the LMS® modal analysis package. These mode shapes are shown in fig. 11, with a special attention to the 2^{nd} and the 5^{th} mode shapes of torsional characteristic. A good agreement was found between the numerically predicted and the experimentally identified modal parameters, with a small difference.

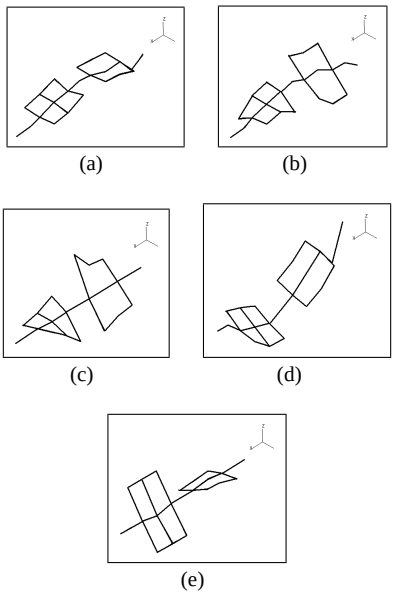

Figure 11: The experimentally identified mode shapes of the scanner. (a) 1^{st} mode - 658 Hz (b) 2^{nd} mode - 1357 Hz (c) 3^{rd} mode (torsional) - 1248 Hz (d) 4^{th} mode - 2269 Hz (e) 5^{th} mode (torsional) - 2518 Hz

Using the FEA results of the mode shapes, it was observed that the mode shapes 2 and 4 are characterized by in-plane displacements of the scanner. Therefore, it was not possible to measure these modes accurately using the LDV as it measures the out-of-plane velocity field only. Nevertheless, some velocity components were detected and these two mode shapes were identified but they could not be conclusive.

5. Analysis

Figure 12 presents the FEA predicted modes and the experimental torsional modes of the device, the most important modes in this kind of device. According to this figure the measured mode shapes are in good agreement with the FEA predicted ones. Observe that the experimentally identified mode shapes could be related to the fact of using a macro-sized LDV with a relative big beam spot, when compared to the scanner dimensions. Better experimental analysis could be conducted by using a specific micro LDV, suitable for MEMS.

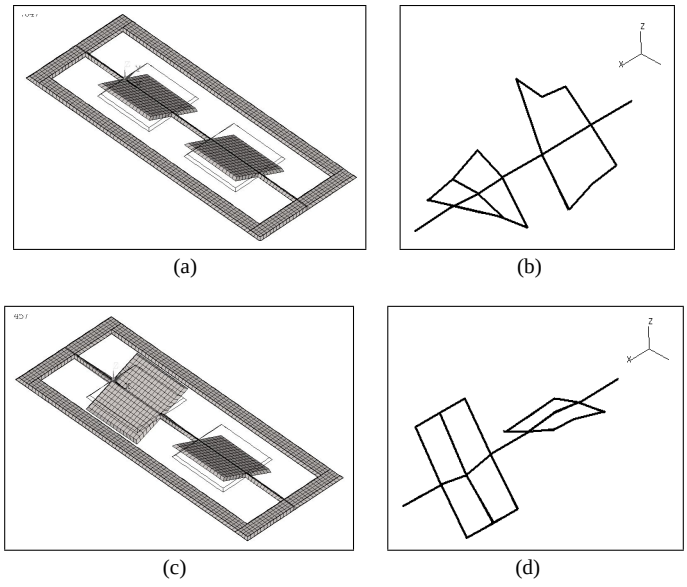

Figure 12: FEA predict and experimental torsional modes of the device.

In tab.5 is presented a comparison between the FEA predict and the measured frequencies. The FRF results presents the frequency of the odd modes of the structure. The 3^rd and 5^{th} modes are torsional modes and their frequencies are in good agreement with the experimental results obtained.

Table 5: Results comparison between the FEA, LDV and Frequency Response methods.

Results Comparison			
	FEA [Hz]	**LDV [Hz]**	**Freq. Resp. [Hz]**
1st mode	677	658	-
2nd mode	1130	1357	-
3rd mode	1595	1248	1316
4th mode	2528	2297	-
5th mode	2765	2518	2542

6. Conclusions

In this work a reliable FEA model of the double-rotor scanner was implemented . The predict dynamical behavior of the device was in agreement with the measured frequency response test and the modal identification performed by laser doppler vibrometry. The torsional modes, the most important in such kind of device, were predicted with an error smaller than 15%. The accuracy of this model can be improved if the orthotropic properties of the Silicon were included in the model.

7. Acknowledgments

This work was partially supported by FAPESP under project $00/10487 - 4$ and CNPq (MCT), process number $14040 - 5/2002$. The authors are grateful to Carolina, Júlio, Marcio and Mariana for their help in this project and to CCS/UNICAMP for the microfabrication facilities.

References

Barbaroto, P. R. ,2002, “Projeto, Microfabricação e Caracterização de Defletor de Luz de Silício Acionado por Indução.”, Master’s thesis, Faculdade de Engenharia Elétrica e Computação - UNICAMP, Campinas, SP.

Kovacs, G. T. A., Maluf, N. I., and Petersen, K. E. ,1998, “Bulk micromachining of silicon.”, Proceedings of IEEE, Vol. 86 No. 8 pp. 1536–1551.

Miyajima, H., Asaoka, N., Isokawa, T., Ogata, M., Aoki, Y., Imai, M., Fujimori, O., Katashiro, M., and Matsumoto, K. ,2003, “A MEMS electromagnetic optical scanner for a commercial confocal laser scanning microscope.”, Journal of microelectromechanical systems, Vol. 12 No. 3 pp. 243–251.

Oliveira, L. C. M. and Ferreira, L. O. S. ,2003, “Silicon Micromachined Double-Rotor Scanner.”, Proceedings of SPIE, Vol. 21 No. 3 pp. 634–642.

Petersen, K. E. ,1980, “Silicon torsional scanning mirror.”, IBM J. Res. Develop., Vol. 24 No. 5 pp. 631–637.

Seidel, H., Csepregi, I., Heuberger, A., and Baumgartel, H. ,1990a, “Anisotropic Etching of Crystalline Silicon in Alkaline Solutions.”, J. Eletrochem. Soc., Vol. 137 No. 11 pp. 3612–3626.

Seidel, H., Csepregi, I., Heuberger, A., and Baumgartel, H. ,1990b, “Anisotropic Etching of Crystalline Silicon in Alkaline Solutions. II - Influence of Dopants.”, J. Eletrochem. Soc., Vol. 137 No. 11 pp. 3626–3632.

Urbach, J. C., Fisli, T. S., and Starkweather, G. K. ,1982, “Laser scanning for electronic printing.”, Proceedings of IEEE, Vol. 70 pp. 597–618.

Williams, K. R. and Muller, R. S. ,1996, “Etch Rates for Micromachining Processing.”, Journal of Microelectromechanical Systems, Vol. 5 No. 4 pp. 256–269.

Wu, M. C. ,1997, “Micromachining for optical and optoelectronic systems.”, Proceedings of IEEE, Vol. 85 No. 11 pp. 1833–1856.

Zeleny, R. ,2004, “Scanning the Scene.”, SPIE´s OEmagazine, pages 30–32.

8. Responsibility notice

The authors are the only responsible for the printed material included in this paper.